

Atomically resolved nucleation and initial growth of a Ag three-dimensional island on Si(001) substrate

Osamu Takeuchi,^{1,*} Masami Kageshima,² Hiroshi Sakama,³ and Akira Kawazu⁴

¹*Institute of Applied Physics, University of Tsukuba, Tsukuba, Ibaraki 305-8573, Japan*

²*Department of Physics, Tokyo Gakugei University, Koganeishi, Tokyo 184-8501, Japan*

³*Department of Engineering and Applied Sciences, Sophia University, 7-1 Kioi-cho, Chiyoda-ku, Tokyo 102-8554, Japan*

⁴*School of Science and Engineering, Tokyo Denki University, Chiyoda-ku, Tokyo 101-8457, Japan*

(Received 6 October 2010; published 31 May 2011)

The initial growth of a Ag three-dimensional island on an atomically resolved Si(001) substrate was investigated *in situ* by scanning tunneling microscopy (STM) at room temperature. It took ~ 20 min for the island to grow from nucleation to a final dimension of $25\text{ nm} \times 35\text{ nm} \times 22$ monolayers (ML). Uniquely, the island growth occurred under no Ag deposition. The Ag atoms required for the growth were provided from the two-dimensional Ag layer and diffusing Ag atoms on the layer that was deposited before the observation. Thanks to this unique growth mechanism, it was allowed to observe the island growth under an isotropic supply of Ag atoms without the shadowing effect of metal deposition by a scanning probe. On the other hand, the STM measurement itself affected finite effects on the growth; attractive interaction between the probe and Ag atoms promoted nucleation of the island, and tunnel current injection may have increased the effective temperature of the system. Despite such a measurement effect, some growth processes that are characteristic of typical metal thin-film growth on silicon substrates were clearly visualized, such as anisotropic and nonmonotonic growth rates that were affected by atomic surface defects, and the growth mode transition from area oriented to height oriented due to an accumulation of stress arising from the lattice mismatch.

DOI: [10.1103/PhysRevB.83.205433](https://doi.org/10.1103/PhysRevB.83.205433)

PACS number(s): 68.55.A–

I. INTRODUCTION

The initial growth of metal films on semiconductor substrates has been the subject of much interest for scientists for decades. In particular, molecular beam epitaxy (MBE) of metal film in ultrahigh vacuum is regarded as a model case where metals grow in the best-controlled environment. It exhibits many fascinating physical phenomena such as adsorption of metal atoms, diffusion, segregation, nucleation of nanocrystals, growth, incorporation, and so on. Such nanoscale physics often influence the macroscopic properties of the film being grown. In many cases, the property of the interface between the film and the substrate is also determined at this stage, because the initial stage of the metal film growth coincides with the formation of the metal-semiconductor interface.

Particularly on Si substrates, metal thin films often grow in a Stranski-Krastanov mode (SK mode), where the growth occurs as follows. First, the deposited metal atoms diffuse over the clean substrate surface as single atoms and then as nanometer-scale clusters. The cluster size gradually increases and when it exceeds some threshold, the cluster settles at one place and acts as the nucleus of an island of two-dimensional (2D) monoatomic layer. Such nuclei grow, absorbing the diffusing adsorbates in the neighboring region, merge with other 2D islands, and eventually cover the whole surface. In some systems, additional adsorption causes the phase transition of the 2D layer from a low atomic density phase to a high atomic density phase. Once the whole surface is saturated by the 2D layer of the highest atomic density, excess adsorbates diffuse over the 2D layer. When the adsorbates' size exceeds some threshold, nucleation of a three-dimensional (3D) island with a height of several atomic layers occurs. The 3D islands

grow, absorbing the adsorbates diffusing in the neighboring regions, and touch and merge with other 3D islands. Finally, the whole surface is covered by the metal thin film that is made of an aggregation of the grown 3D islands.

To observe thin-film growth at such a microscopic level, scanning electron microscopy (SEM) and low-energy electron microscopy (LEEM) have been widely used. Such techniques are especially useful for observing the growth process *in situ*, thanks to their fast imaging rate and their nanometer-scale resolution.^{1–3} However, techniques using an electron beam as the probe cannot measure the accurate height of the 3D islands nor the atomic defects on the substrate surfaces. In contrast, scanning tunneling microscopy (STM) offers the means to observe the surface morphology with atomic resolution as well as an accurate height profile. In an STM measurement, however, several technical difficulties exist. One is that the tip and the scanner of the STM probe create a shadowing effect of the molecular beam during *in situ* observation of the film growth with a gradient incidence of the molecular beam. Second is the slow scan rate of STM. This makes the observation of a fast process such as the nucleation of the 3D island difficult. Third is the measurement effect due to the strong interaction of the scanning probe with the measured system. Injected tunnel carriers give finite energy into the system and raise the effective temperature in the localized area. Electrostatic interaction and van der Waals' forces that exert between the tip and the adsorbates affect both the local density and effective mobility of the adsorbates.

In this paper, we studied a unique epitaxial system of Ag film grown on Si(001) by STM at room temperature. As discussed below, in this system, the Ag 3D island spontaneously grew without Ag deposition. This unique growth condition eliminated the first difficulty of the shadowing effect.

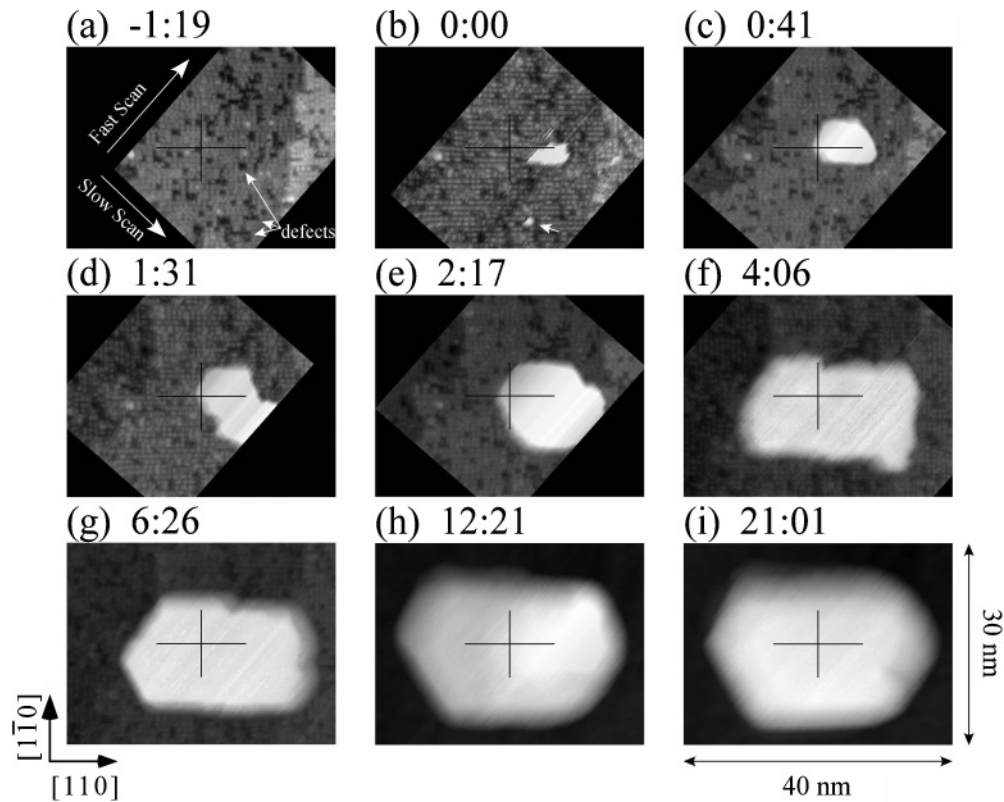


FIG. 1. Series of STM topographic images measured on a supersaturated Ag 2D layer. Spontaneous nucleation and initial growth of a Ag 3D island was observed *in situ* for ~ 20 min. The measurement time for each image is displayed above. Measurement conditions: reference tunnel current of 0.3 nA and sample bias voltages of (a) -1.5 , (b) 1.0 , (c) -1.0 , (d) 1.5 , (e) -1.5 , and (f)–(i) 1.5 V. The black cross indicates the center of the image.

A scan-line-oriented precise analysis of a STM image revealed the nucleation process in several tens of milliseconds, which was turned out to be strongly affected by the measurement. Nevertheless, according to a careful evaluation of the measurement effect, several physical phenomena that are characteristic of typical metal thin-film growth on a silicon substrate were recognized.

Because of the weak reactivity of Ag with Si, Ag films on Si are known to have an atomically sharp interface between the film and substrate when deposited at room temperature. Thus, this system has been regarded as a model system of a metal-semiconductor interface.⁴ Among numerous studies on Ag/Si(111), there are relatively few which examine 3D Ag growth on Si(001).^{5–9} Among them, there is an interesting report by Glueckstein *et al.*⁸ They reported that the growth of the 3D island in this system is accompanied by the “unwetting” of the 2D Ag layer. Namely, as in normal Stranski-Krastanov growth,¹⁰ the 2D layer growth is completed before the initiation of the 3D island growth. However, during the growth of the 3D islands, some of the Ag atoms leave the 2D layer and go into the 3D islands, resulting in the exposure of areas of the original clean Si surface. Glueckstein *et al.* determined the areas that were covered by the 2D layer before and after initiation of the 3D island growth and found that the area was smaller after the 3D island growth even though more Ag had been deposited on that surface. The unwetting phenomenon indicates that the free energy for the Ag atom in the 3D island is lower than that in the 2D layer and that the energy barrier

for the migration is reasonably low. In the present study, we analyzed the spontaneous growth of the Ag island without additional deposition on a supersaturated 2D layer of Ag on Si(001) at room temperature.

II. METHOD

The experiment was carried out with an ultrahigh vacuum (UHV) STM system. The Si(001) substrate was flash cleaned and cooled down ~ 1 h before the experiment. It was then placed on the STM sample stage and Ag was deposited for 1 min from a tungsten filament onto the Si(001) substrate at room temperature. The deposition rate had previously been calibrated to be ~ 1 monolayer (ML)/min. Thus, the estimated coverage was 1 ML, exactly the same as the saturation coverage of the Ag 2D layer on Si(001) at room temperature. Here, $1 \text{ ML} = 6.78 \times 10^{14} \text{ cm}^{-2}$, the atomic density of the Si(001) surface. During deposition, the STM tip was retracted from the sample by a few millimeters to avoid blocking the Ag atoms. After deposition, a sequence of STM topographic images was taken at room temperature without additional Ag deposition.

III. RESULTS

A. Growth of 3D island

Figure 1 shows some of the STM topographic images from the 15 sequentially obtained images. It took ~ 20 min to complete all the images, as indicated by the measurement

time written above each image. During the measurement, a 3D island of Ag grew from the nucleus in Fig. 1(b), with dimensions of a few nanometers, to the single crystal of dimension $25 \text{ nm} \times 35 \text{ nm}$ shown in Fig. 1(i).

These images were originally taken under a variety of measurement conditions. The scanning area and scanning velocity differed from image to image. Thus, prior to the analysis, each image was rotated and a linear drift correction was applied. Then, the relative position of the images was carefully determined, referring to the atomic defects on the substrate, hence, exactly the same area of the sample is displayed in all the images in the figure. The black crosshair indicates the center of each image. The scan direction of the original image is as indicated in Fig. 1(a). During the measurement, no additional Ag was deposited. Instead, the island grew spontaneously, consuming the Ag atoms in the 2D layer on this surface, as previously suggested and identified as the “unwetting” process.⁸ Since the present growth process occurred under a finite measurement effect, we will revalidate this interpretation later.

Now, let us look into the growth of the 3D island in detail. Figure 1(a) shows the surface before the nucleation. A Ag coverage of 1 ML was reported as the saturation coverage of the 2D layer for room-temperature deposition.¹² In accordance with the report, while the surface is apparently fully covered by the 2D layer, scans over the larger area of this sample showed no Ag 3D islands. Previously, two different structures were reported as 2D layer structures of Ag on Si(001) deposited at room temperature. Both are not very well ordered structures, but one has 2×1 and 2×2 local periodicity,^{11,12} and the other has a local periodicity with a ringlike structure.¹³ According to our study, the former structure appears when the substrate is at room temperature while the latter structure appears when the substrate is not completely cooled down after flash cleaning.¹⁴ The threshold temperature is estimated below 400 K. In this study, we cooled down the sample after flashing for $\sim 1 \text{ h}$; the former structure was dominant on the surface while the latter structure was also found in some places. The depressions, some of which are indicated by the arrow in Fig. 1(a), are the missing dimer defects which originally existed on the clean substrate. As reported,^{6,8,15} such defects strongly prevent the growth of the Ag 2D layer on them. Thus, effective saturation coverage of the 2D layer depends on the defect density. Namely, when the entire surface, except for the defect sites, is fully covered by the 2D layer with a Ag density of 1 ML, the 3D island starts to grow. We prepared this exactly saturated surface by various trial-and-error iterations by adjusting the deposition time.

As was pointed out previously,^{11,12,15} an unsaturated 2D layer of Ag shows a considerable amount of noise in the STM images that appears as horizontal discontinuities aligned with the scanning direction. Even on our saturated surface, some noise was seen, especially in the area with the local 2×1 periodicity, indicating low-frequency thermal fluctuation of the surface structure at room temperature. In addition, we noticed a noise that appears as much brighter streaks, unrelated to the 2D layer structure. We interpreted this noise as an indication of excess Ag atoms diffusing over the 2D layer. This surface is considerably unstationary even at room temperature.

In Fig. 1(b), the nucleation of the Ag 3D island occurred, which appears as the bright region in the middle of the image.

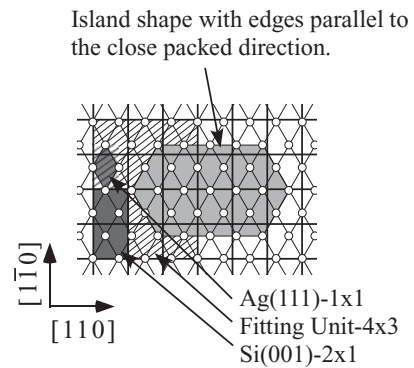


FIG. 2. Schematic of the lattice matching between the Ag(111) 3D island and substrate Si(001). A 4×3 cell of Si(001) matches a rectangular 6×4 cell of Ag(111). The direction of the characteristic linear edges of the Ag 3D island observed in Fig. 1 is parallel to the close-packed direction of the Ag(111) surface. The mismatch is 0.2% along Si[110] and 2.2% along Si[1-10].

Its outline has a sharp linear edge on the upper left-hand side, which is parallel to the scan line. This linear edge does not indicate the real shape of the island but is caused by the line-by-line manner of the STM measurement; the island did not exist before this scan line was measured. We will discuss this point later in detail. There is another small Ag cluster, which abruptly appeared in the lower part of this image, indicated by the white arrow. Its lateral dimension was more than 1 nm and its height was $\sim 0.3 \text{ nm}$. This particle disappeared in the next image, as shown in Fig. 1(c). This indicates that the critical size for 3D island nucleation is larger than the size of this particle, at least under the finite perturbation due to the STM observation.

In Figs. 1(c)–1(i), the Ag island that nucleated in Fig. 1(b) grows to become a 3D island with a lateral dimension of $25 \text{ nm} \times 35 \text{ nm}$ and a height of more than 20 ML in $\sim 20 \text{ min}$.

While the footprints of the smaller islands were rather irregular, those of the larger islands tended to have linear edges that crossed each other at 120° , one of which was parallel to Si[110]. Hereafter, we denote the Si dimerization direction on the central Si terrace as [1-10] and the dimer row direction as [110]. According to the edge direction, the crystal orientation of the Ag island was estimated to be Ag(111)//Si(001) and Ag[1-10]//Si[110], which is consistent with previous reports.⁹ The lattice-matching condition of Si(001) and Ag(111) for this orientation is shown in Fig. 2. Generally, Ag/Si is a large lattice-mismatch system; the surface lattice constant of Ag(111) is 0.289 nm and that of Si(001) is 0.384 nm. However, the system has a matching condition where a 4×3 cell of Si(001) corresponds to a rectangular 6×4 cell of Ag(111), as shown in the figure. In this matching, the Ag lattice is 0.2% larger along Si[110] but 2.2% smaller along Si[1-10]. The smaller mismatch along Si[110] explains why the observed island is elongated in this direction.

The small islands had almost atomically flat top surfaces, despite the irregular shapes of their footprint. The larger islands also had flat top surfaces, though the edge parts were slightly beveled. Thus, the irregular footprint does not seem to be due to the growth of twinned or multiply twinned crystals. This is in contrast to the Ag growth on the H-terminated Si(001)

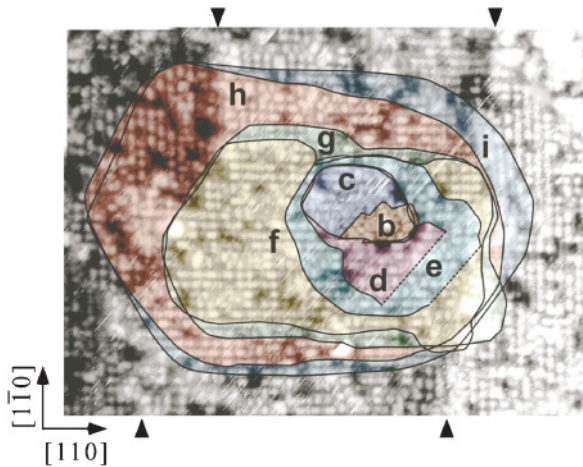


FIG. 3. (Color) Evolution of the Ag 3D island's footprint superimposed on a synthesized image of the substrate atomic structure. The substrate structure was reconstructed from Figs. 1(a), 1(b), 1(e), 1(f), and 1(g). The black arrowheads indicate the single atomic steps on the substrate.

substrate, where the formation of multiply twinned crystals was reported.³ The reason for the irregular footprint as well as for the anisotropic and nonmonotonic growth mode of the island can be interpreted in terms of the atomic structures of the substrate as follows.

Figure 3 shows the synthesized atomic structure of the 2D layer beneath the island and the evolution of the 3D island's footprint on it. Since no single image covered the entire area of interest, we synthesized this image by merging parts of Figs. 1(a), 1(b), 1(e), 1(f), and 1(g). On this surface, many missing dimer defects are observed in addition to the two single atomic steps that are indicated by the two sets of black arrowheads. Each footprint is of the measured island in the corresponding STM image shown in Fig. 1, as indicated by the letters (b)–(i). Determining the island's footprints from the STM images can be a little controversial. When the island is tall, the island tends to be imaged larger in the lateral dimension than its real shape due to the finite radius of the STM tip apex. In general, the island shape in a STM image is determined by the convolution of the sample and tip shapes. For simplicity, in this study, we drew the outline where the topographic gradient is largest. Due to the tip shape effect, the estimated footprints might be slightly larger than that of the real island. In Figs. 1(d) and 1(e), the island extended out of the scanned area. For these images, the broken lines indicate the border of the scanned area.

According to Fig. 3, it can be seen that the growth was quite anisotropic and nonmonotonic. At first, the island grew toward the upper left-hand side in Fig. 3(c) but toward the lower right-hand side in Fig. 3(d). Then it grew rather isotropically in Fig. 3(e), toward the left-hand side in Fig. 3(f), isotropically in Fig. 3(g), to the left-hand side in Fig. 3(h), and to the right-hand side in Fig. 3(i). It can be seen that the anisotropy was due to the surface irregularity, i.e., missing dimer defects and atomic steps, as follows. The right-hand part of the island outline in Fig. 3(b) was surrounded by three large defects on the substrate. Then, the outline in Fig. 3(c) was surrounded by defects in all directions. In contrast, no defects existed in the

area surrounded by the outline in Fig. 3(c), i.e., at the interface between the substrate and the Ag island in Fig. 3(c). This suggests that the surface defects prevent the island growth. Since the island in Fig. 3(c) was completely surrounded by defects, the island must have extended over some defects for further growth. In Fig. 3(d), the island grew over the large area with less defect density in the lower right-hand direction. In Fig. 3(e), the island had grown almost isotropically. In the upper right-hand part, however, the growth was stopped by the existence of the defect, resulting in a kink in the outline. In Fig. 3(f), the island had grown in the Si[110] direction much more than in the Si[1-10] direction. As discussed above, this can be explained by the lattice mismatch. More specifically, however, it had grown toward the left-hand side but not toward the right-hand side. Indeed, both the left- and right-hand edges of the island in Fig. 3(f) were on single atomic steps of the substrate. This suggests that the step edges also prevent the island from growing. Due to these constraints, the outline of the island in Fig. 3(f) is still irregular as compared to the larger islands. In contrast, when the island grew large enough, its shape tended to have crystallographically preferred directions. The height of the island doubled from Fig. 3(g) to Fig. 3(h). As the height increases, the gain in free energy to have crystallographically preferred edges overcame the loss to have the island's footprint over the step edges and atomic defects.

It is notable that the footprint of the island did not always extend but sometimes shrank in part. The lower right-hand part of the island in Fig. 3(f) and Fig. 3(g) disappeared in Fig. 3(h). Even when the island was larger, the upper left-hand part of the island in Fig. 3(h) disappeared in Fig. 3(i). As seen later, when the island footprint contracted, the island height increased instead. Thus, the apparent nonmonotonic growth was, in reality, the transformation of island shape. If the substrate temperature is high, liquid deformation can cause such a transformation. In the present case, however, the system temperature is so low that the crystal structure of the island is in a solid phase. This can be seen from the fact that stable STM measurements were possible on the island. Consequently, liquid deformation is not likely to happen. Instead, we suggest that a high surface mobility of Ag atoms in this system causes the transformation. The high mobility of the Ag adsorbates causes the active exchange of Ag atoms between the three different phases of Ag, i.e., the 2D layer phase, the 2D gas phase of the free adsorbates diffusing over the 2D layer, and the 3D island phase. Transformation of the island occurs via emission of Ag atoms from an unstable part of the island and absorption of Ag atoms in an energetically favorable part. To date, there has been a theoretical study on the surface diffusion of Ag adatoms and Ag dimers on the clean Si(001) substrate,¹⁶ in which diffusion barriers of ~ 0.5 eV were found. To the best of our knowledge, there have been no reports of theoretical predictions for the diffusion barrier of Ag atoms on the Ag 2D layer.

Next, we investigate the growth rate of the island quantitatively. Figure 4(b) shows the evolution of the area and height of the island as a function of the measurement time. Figure 4(a) shows the number of the Ag atoms contained in the island, which was estimated by the volume of the island and the atomic density of the bulk Ag. In some images, the

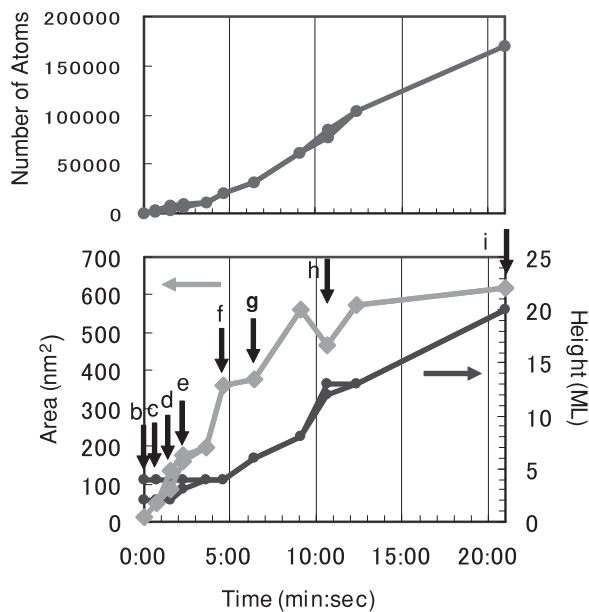


FIG. 4. Time evolution of the height and area of the Ag 3D island and of the number of Ag atoms contained in the island. Measurement points corresponding to the STM images shown in Fig. 1 are marked by the letters (b)–(i). While the height (bottom, black line) increased linearly, the area (gray line) reached saturation due to the accumulation of stress arising from the lattice mismatch.

island extended outside of the measurable range. In such cases, two points are plotted; one is the minimum value confirmed in the image as the lower limit and the other is the value found in the next measurable point as the reasonable upper limit. The true value is supposed to exist between these two.

In this range of the measurement time, the height of the island increased almost linearly while the area was saturated at $\sim 9:00$. Consequently, the number of atoms increased as a square function until $9:00$ and then as a linear function. In the simplest model, when we assume that the absorption rate of the diffusing Ag atoms by the 3D island is proportional to the length of its footprint's boundary, the increase of the volume growth rate should be proportional to the square root of the footprint area. In the experiment, however, the increase rate of the volume was much larger, almost proportional to the footprint area. We have not found a good explanation for this fact.

The saturation of the footprint area at $\sim 9:00$ occurred after the left-hand side boundary crossed over the left atomic step. Thus, it seems to be due to the accumulation of stress from the lattice mismatch. Even after this point, the increase rate of the height was almost constant. At the last measured point at $21:01$, the height was 5.2 nm, which was much smaller than the shorter width of the island, ~ 25 nm. Thus, the increase of the surface free energy on the sidewall of the island might not have affected the growth up to this moment. Although it would have been very interesting to see how long this constant growth rate is maintained, unfortunately, the STM tip broke after the measurement shown in Fig. 1(i). Here, we remind that the measured growth rate might be affected by the measurement effect due to the STM scan. We will review this point later.

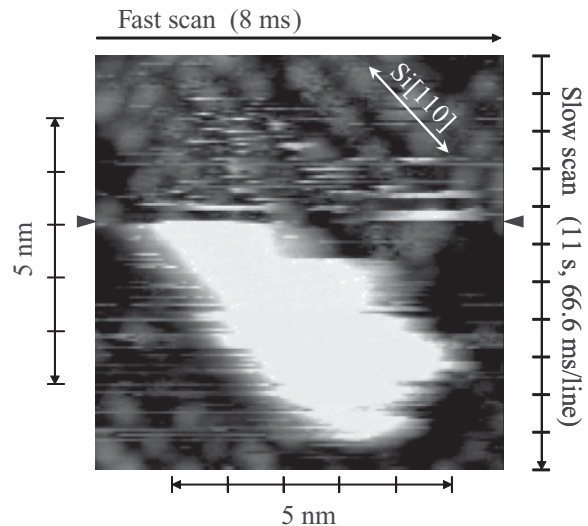


FIG. 5. Magnified image of Fig. 1(b). Since the STM image is measured line by line, the lateral axis of the image can be interpreted as the time scale as well as the distance scale. The black arrowheads indicate the scan line where the nucleation occurred.

B. Nucleation of 3D island

Next, we look into the nucleation process observed in Fig. 1(b) in detail. As discussed later, however, the precise analysis of the image indicates the existence of strong perturbation to the nucleation process by STM measurement. Thus, do not take the following results directly as the intrinsic behavior of the Ag atoms in this system. Figure 5 shows part of the STM image. This image was not rotated and the drift was not corrected after measurement. In general, a STM image is measured in a line-by-line manner. Thus, different pixels in the image are measured at different times. In this sense, the vertical and horizontal axes of this image can be regarded as the time scale as well as the distance scale. It took 8 ms to scan the area in this image from the left-hand side to the right-hand side, while it took 33 ms for one way and 66 ms for a roundtrip to scan a whole scan line. Thus, it took ~ 11 s to scan the displayed 166 lines from top to bottom. From this figure, we can determine the moment of the nucleation at the scan line, indicated by the two black arrowheads.

Figure 6 shows a more detailed figure, in which 60 scan lines around the nucleation were magnified from Fig. 5. Six characteristic scan lines are marked in different colors and the corresponding line profiles are plotted below. In this experiment, the height signals above 0.62 nm and below 0.14 nm, which are indicated by the broken lines in the figure, were not measured correctly due to the saturation of the analog-to-digital converter (ADC). Thus, the flat regions appearing in the line profile at these levels are not the true profile of the sample surface.

The scan line marked by the light blue color corresponds to the moment of nucleation. After this line, the Ag 3D island was observed continuously whereas it did not exist before. The measurement times for the six marked lines are displayed using the nucleation time as the origin. The scan lines measured before the nucleation contain a number of short bright streaks parallel to the scan lines, some of which are marked by white

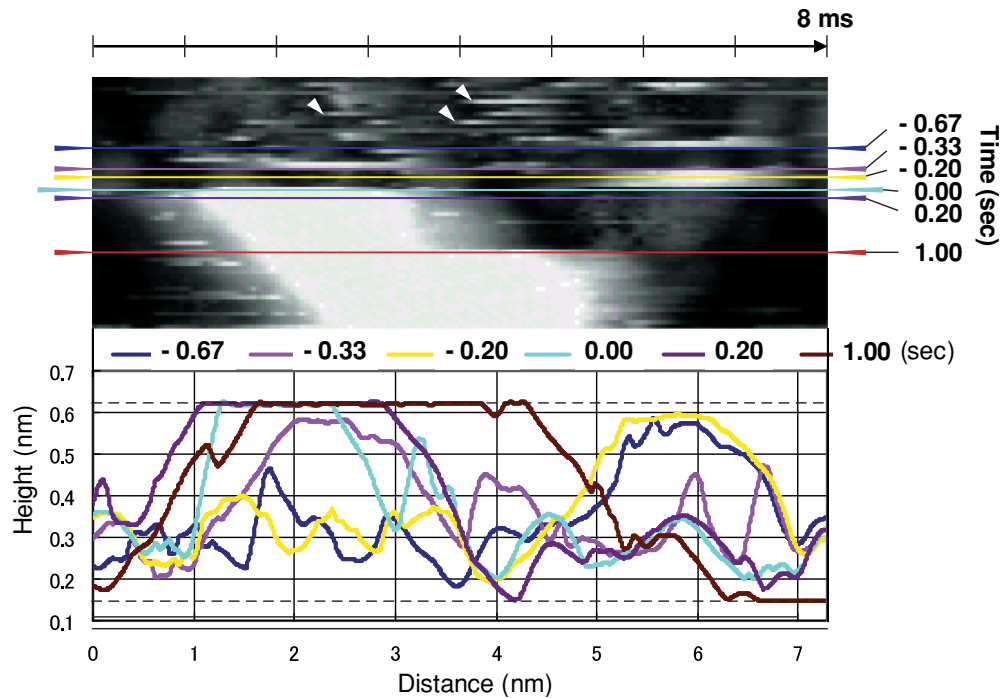


FIG. 6. (Color) Further magnified image of Fig. 5. The 60 lines around the nucleation are displayed. The hopping of a Ag cluster and nucleation of the island were observed over a time scale of several tens of milliseconds. Six scan lines are marked and discussed in the main text and the corresponding line profiles are displayed in the lower plot. In the plot, the two broken lines indicate the window of the ADC used in the STM electronics. The values out of this window were clipped, resulting in the artificial flat region in the plot.

arrowheads. These bright lines indicate the existence of Ag atoms or clusters diffusing over the Ag 2D layer. Before -0.80 s, which is two lines before the blue mark, all the bright lines appeared individually, i.e., not continuously in the direction perpendicular to the scan line. This means that the Ag clusters did not stay at the same place for more than twice of the scan line period. The length of the bright line in the scan direction is determined either by the actual size of the cluster or by its resting time. Regarding the latter, it is also affected by the bandwidth of the current-voltage preamplifier and that of the z -piezo feedback loop of the STM system. In the present case, the former was ~ 10 kHz and the latter was < 1 kHz. Thus, it is difficult to establish which factor determined the length of each bright line.

After -0.80 s, some of the Ag clusters stayed at the same place for more than two scan lines. On the blue line, a cluster was located at 5.8 nm on the horizontal axis. This cluster appeared two lines before the blue line when the tip was scanning at ~ 6.1 nm and disappeared after the blue line was scanned. The next stable cluster was observed at ~ 2.4 nm along the magenta line. This cluster appeared two lines before the magenta line when the tip was at ~ 3.0 nm and disappeared after the magenta line was scanned. In between, for almost three scan lines, no stable clusters were observed. On the magenta line, when the tip was at ~ 6.6 nm, a cluster appeared again at ~ 5.8 nm, as shown along the yellow line, which disappeared just before the light blue line. On the light blue line, a cluster appeared at 2.0 nm and at that position the nucleation of the island occurred.

According to the line profiles, the clusters that appeared twice at 5.8 nm and once at 2.4 nm between those two had

almost the same size, both with regard to width and height. It is natural to believe that the same cluster hopped back and forth between these two sites. The width of the cluster was ~ 1.6 nm and its height was ~ 0.3 nm, which was slightly larger than the single atomic step height on the Ag(111) surface, 0.23 nm. Thus, the cluster was estimated to be 2 ML high, including the Ag layer in the 2D phase. When the nucleation occurred, the height of the island was higher than the hopping cluster. Although the exact height was not obtained due to the saturation of the ADC, it can be fairly estimated as 3 ML. Since the left-hand side edge of the island on the light blue line showed an unrealistic steep gradient, that part might not reflect the cluster shape. Rather, it is likely that the cluster hopped into this site when the tip was scanning at ~ 1.0 nm. In the same way, the depression ~ 3.0 nm can be explained by the hopping of the cluster. At this moment, the cluster disappeared for a short while and soon appeared again. The small depression ~ 3.4 nm might be also due to the hopping. This explanation is consistent with the fact that the envelope of the light blue line coincides with the purple line, which was observed two scan lines after the nucleation. If this is the case, the nucleation occurred when the 3-ML-high cluster stopped moving, staying in one position. Thus, it is difficult to know the minimum size of the nucleus because the light blue line does not show the actual shape. If the size was the same as that of the purple line, its height was 3 ML and its width 2.6 nm.

Since the island grew continuously even as parts of it were scanned, it is difficult to estimate the dimension of the initial nucleus perpendicular to the scan line. For example, at the brown line, the width of the island abruptly increased. This indicates that the island grew considerably after the

previous line was scanned. Thus, the nucleus should have been much smaller than the apparent size of the island observed in Fig. 1(b). To further discuss the size and shape of the initial nucleus, we may gain some clues from observing the Ag cluster marked by the white arrow in Fig. 1(b). We noticed that the size and shape of this cluster were almost identical to those of the cluster observed in the line profiles in Fig. 6. They were also similar in the fact that both of them easily hopped around the surface. So, we suggest that they may be typical of the type of Ag clusters diffusing on this surface. Although the shape of the cluster perpendicular to the scan line is not evident in Fig. 6, this cluster almost fully exposed its shape in the image. According to the image, the cluster, and supposedly the other cluster investigated in Fig. 6, had simple circular shapes. Thus, the initial nucleus would have formed from either one such cluster that had grown a slightly more or a few of these incorporated clusters. In summary, it was observed *in situ* that Ag clusters 1.6 nm wide and 0.3 nm high were hopping around on this surface before nucleation. When the cluster grew to be 2.5 nm wide and 0.4–0.5 nm high, it became the initial nucleus of a 3D island.

Next, let us examine the substrate structure below the nucleus. Figure 7(a) shows part of Fig. 1(b), which is colored in red where the topographic height is larger than 0.4 nm. Figure 7(b) shows the STM image measured over the same area before nucleation, with the same area shaded in red. Since different bias voltages were applied for these two images, the 2D layer surrounding the island appears quite differently. However, if the bias voltage dependence is taken into account, the surface structure itself is identical in both images. Two black circles mark the positions where the Ag cluster favorably stayed. According to the image, the surface structures at these positions were not distinguishable from that of other places. An ordinary Ag 2D layer was found there.

C. Measurement effect on nucleation

Here, we mention that the observed behavior of the Ag atoms or clusters about the nucleation have been strongly affected by the STM measurement. In order to understand it, we first review the possible measurement effects that affect the growth process and then interpret the experimental result. The STM measurement can affect the growth in two different ways. One is via the energy injection into the system brought by the tunnel current. In the present study, the typical measurement condition was a tunneling current of 0.3 nA and a bias voltage of 1.5 V. Consequently, if the whole energy is consumed to elevate the system temperature of an atomically localized region beneath the probe, the effective temperature will be extremely increased. In reality, however, most of the injected electrons tunnel the vacuum gap elastically and flow the surface region ballistically within the mean free path. Thus, the actual energy dissipation occurs in a relatively wide region in the substrate, whose dimension is comparable to the mean free path of the tunnel carrier, several tens of nanometers at room temperature. At the same time, a very small portion of the injected carrier tunnels the surface area inelastically, giving energy to the very local area beneath the STM probe. Consequently, the energy brought by the tunnel current increases the averaged system temperature in

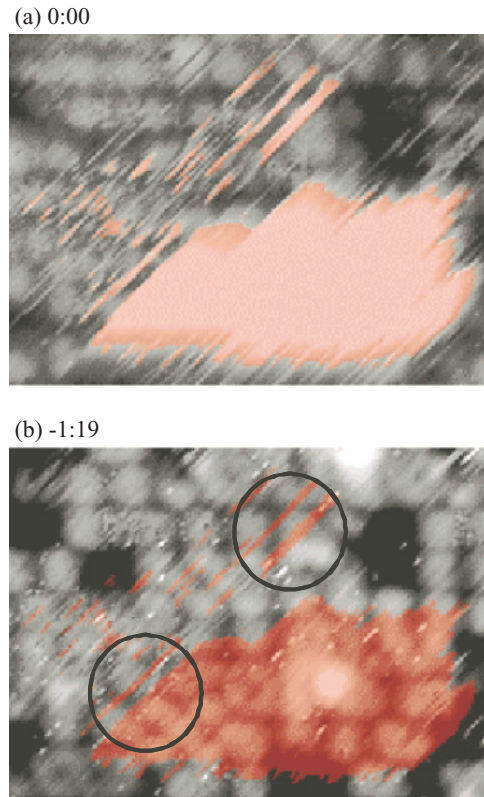


FIG. 7. (Color) Magnified images of (a) Fig. 1(b) and (b) Fig. 1(a). The same regions are colored in red. Two black circles indicate the positions where the Ag clusters stayed favorably. The atomic structure of the substrate at these points was not distinguishable from other regions. See the main text for detail.

the scanned region due to the former process and increases the mobility of the adsorbate just under the probe due to the latter process.

The STM measurement can also affect the growth via direct interaction between the probe and the adsorbates. Possible interactions are the electrostatic interaction and van der Waals' interaction. Such interactions have been already well investigated and sometimes they are utilized to manipulate the atoms, molecules, or clusters with the STM probe.¹⁷ For instance, van der Waals' interaction between the probe apex and a neutral adsorbate results in an attractive interaction. In contrast, the electrostatic interaction between two dipoles, one consisting of the substrate and the STM probe with bias voltage applied, and the other consisting of the substrate and the adsorbate with some charge transfer, can be attractive or repulsive depending on the polarity of the bias voltage. A possible long-range interaction due to such an electrostatic force will affect the local density of adsorbates and a possible short-range interaction can pull or push an adsorbate beneath the probe during scan. Note that injection of energy by the tunnel current into the adsorbates in the localized region below the probe might cause an apparent repulsive interaction between the probe and the adsorbates because the excited adsorbates obtain a higher mobility and diffuse away from the probe.

Now, we discuss the major interaction between the STM probe and the adsorbates based on the experimental results.

First, in Fig. 6, the hopping cluster very often hopped into the site being scanned by the STM probe but rarely hopped out of the site being probed. Disappearance of the cluster often occurred while the probe scanned different sites. This suggests some short-range attractive interaction between the probe and the Ag clusters. Long-range attractive interaction was also confirmed by the observation of the same sample surface after measuring the series of images shown in Fig. 1. Although we imaged many other areas on the sample, we found no grown 3D island or any nucleation of another 3D island. That is, no other islands grew at all on the surface. We therefore conclude that we did not observe the nucleation and growth of the 3D island shown in Fig. 1 just by chance. It should be explained by some long-range attractive interaction between the STM tip and the Ag atoms and the clusters. With the interaction, the density of the Ag atoms in the scanned area was increased and the nucleation was caused. If this is the case, the electrostatic interaction exists between the probe and the adsorbates. van der Waals' force will not increase the density of the adsorbates as efficiently because it only exerts on a single adsorbate just beneath the probe. The mobility of the Ag clusters might be increased by the local heating effect of the tunnel current and/or the high electric field between the tip and the sample.

The attractive interaction may also answer why the nucleation occurred at an apparently nonspecific site as observed in Fig. 7. We suggest that not the surface structure at that position but the missing dimer defects surrounding the nucleus may have played important roles. As seen in Fig. 1, the missing dimer defects on the substrate prevented the growth of the Ag island. Therefore, these defects will also work as a barrier for diffusion of the Ag clusters.¹⁸ When the STM tip scans the surface, the Ag clusters will tend to follow the tip motion when the short-range attractive interaction exists. This explains why the hopping often occurred parallel to the scan line. Note that the scan is performed back and forth under the same feedback conditions and velocities in this measurement, although the data acquisition was done only when the tip scanned from the left-hand side to the right-hand side. Since the defects work as a barrier to cluster diffusion, when the tip scans across such a defect, the cluster following the tip will have a relatively high probability of remaining adjacent to the defects.

If the observed nucleation process is strongly affected by the measurement, what can be learned from the present result? Regarding the Ag growth on Si(001), the observed critical nucleus size of 2.5 nm in width and 0.4–0.5 nm in height gives the upper limit of the intrinsic critical size. Without perturbation, a smaller cluster will be stable and act as a nucleus of a 3D island. A measured hopping frequency of clusters with particular sizes also gives the upper limit. If it is allowed to treat the measurement effect simply as the increase of the efficient temperature, at some elevated temperature, Ag clusters with the observed dimension hop and settle as was seen in the present study. On the other hand, preferable hopping directions and preferable adsorbing sites are very likely to originate purely from STM measurement, as discussed above. In order to distinguish the intrinsic behavior of the system from artifacts due to the observation, a future experiment with reduced measurement effect is necessary. One may try to reduce tunnel current and/or adjust the sample bias voltage. We

believe the present result becomes the starting point for such advanced researches. The measurement effect on the island growth after the nucleation will be discussed later.

D. Unwetting of 2D layers

Here, we would like to discuss the transportation of Ag atoms during the growth process. In this study, no Ag deposition was done during the growth of the 3D island. The growth occurred consuming the Ag atoms that preexisted on the surface before the island nucleation. Previously, the 2D layer of Ag grown at room temperature was reported to be unstable and part of it was consumed to form the 3D island during growth.⁸ The consumption of the 2D layer and the resulting exposure of the substrate surface was referred to as “unwetting” of the 2D layer. Here, we investigate whether the Ag atoms required to form the present 3D island was also supplied from the unwetting of the 2D layer or not. Figure 8 shows magnified views of Figs. 1(a) and 1(c) to compare the coverage of the 2D layer adjacent to the island. If unwetting occurs, the coverage should decrease. The island in the figure contains ~ 230 atoms. On the other hand, the Ag density in the 2D layer is 1 ML. Thus, in the displayed rectangular area of 170 nm^2 , including the unscanned black area, there were ~ 1150 Ag atoms in the 2D layer. Consequently, if all the Ag atoms in the 3D island originated only from the displayed area, $\sim 20\%$ of the 2D layer should have been consumed and the bare substrate Si(001) surface would have appeared. In the figure, however, there is almost no noticeable change in the coverage of the 2D layer. In addition, although a very limited area can be compared, the unwetting was not observable for the case of Fig. 1(g), where the island contains $\sim 30\,000$ atoms.

We investigate two mechanisms which would explain this result. One was that the Ag atoms came from a much larger area than what we observed. If we assume that the Ag atoms originated from a $1 \mu\text{m} \times 1 \mu\text{m}$ area, a 0.4% unwetting of the 2D layer will give the 30 000 atoms. Such a small change might not be noticeable in Fig. 1(g). This idea is consistent with the previous observation where the unwetting rate was not dependent on the distance from the grown 3D islands, which are separated from each other by a few hundred nanometers.⁸ The second mechanism was that a large part of the Ag atoms came not from the 2D layer but from the excess Ag atoms

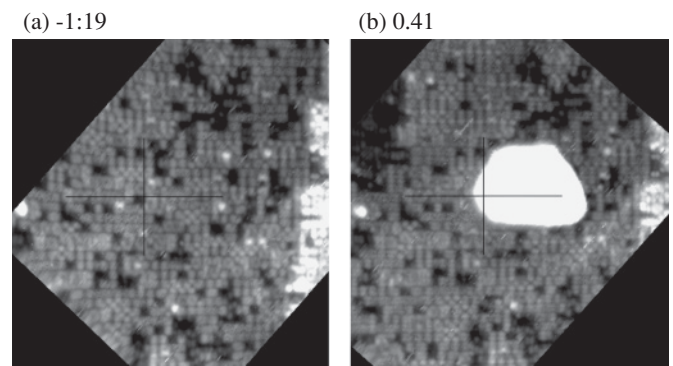


FIG. 8. Magnified images of (a) Fig. 1(a) and (b) Fig. 1(c). Even after the growth of the Ag 3D island, the unwetting of the surrounding 2D layer was not noticeable.

diffusing over the 2D layer, which were not observable in the STM measurement. Note that when the Ag atoms travel over a long distance, such as $1\ \mu\text{m}$, there should be a considerable density of diffusing Ag atoms on the 2D layer. A high density of adsorbates is also required to have a finite possibility for island nucleation. Hence, as discussed above, the island growth process should be described as the active exchange of Ag atoms between three different phases, i.e., the 2D layer phase, the 2D gas phase of the free atoms diffusing over the 2D layer, and the 3D island phase. Before the nucleation of the 3D island, thermal equilibrium was achieved between the 2D layer phase and the 2D gas phase. Once the nucleation occurred, the Ag atoms were transferred from the 2D gas phase to the 3D island phase. Then, the equilibrium between the 2D layer phase and the 2D gas phase was broken and the Ag atoms were transferred between them via the unwetting. Thus, if a sufficient amount of Ag atoms were contained in the 2D gas phase before the nucleation, the 3D island would be able to grow, consuming the atoms in the 2D gas phase without large amounts of unwetting.

Consequently, existence of the unwetting process itself was not confirmed in the present experiment, while it was not denied as well.

E. Measurement effect on island growth

Here, we investigate how much the measurement affected the island growth after nucleation, i.e., the unwetting process of the 2D layer and the growth process of the 3D island. At first, as discussed in the previous section, if the growth accompanies with the unwetting, most of the unwetted sites were distant from the measured region. Since an electrochemically etched W tip, a typical radius whose apex is $\sim 10\ \text{nm}$, was used for the measurement, the interaction between the probe and the 2D layer across several hundreds of nanometers will not be strong enough to cause unwetting. Thus, we insist that the unwetting process, if it exists, is an intrinsic process that occurs without measurement effect.

The measurement must have increased the effective temperature of the system due to energy transfer by the tunnel current and destabilization of adsorbates due to the short-range interaction from the probe. How high can be the effective temperature? It is known that the Ag/Si(001) system exhibits a phase transition of the 2D layer structure from the less-ordered room-temperature phase to a mixture of ordered $c(6 \times 2)$ and 2×3 phase at a temperature between 100 and 200 °C.¹⁹ Thus, the effective temperature was less than this transition temperature. As discussed previously, the heating effect can occur in a very wide area, whose dimension is comparable to the diffusion length of tunneling carriers, while the very local area beneath the probe is strongly heated due to a high density of the tunnel current there. As the probe scans over the surface, the area being heated moves on the surface following the probe. Thus, the amount of the local heating per unit area depends on the measurement area. When a wider area is scanned, the probe scans faster in a wide region. Consequently, the heating effect per unit area becomes smaller. Similarly, the possible artifact of the heating effect on the growth rate will depend on the ratio of the area of the island's footprint to the whole scanned area. In general, a heating effect increases the mobility of adsorbates. Thus, when the probe scans over the island, the

absorption probability of the adsorbates into the island may be reduced. Namely, when the area ratio is larger, a smaller growth rate is expected.

As seen in Fig. 1, the scanned area and the area ratio of the island's footprint differ from image to image. In Fig. 4, the scanned areas were $32 \times 32\ \text{nm}^2$ from 0:00 up to 2:17, $50 \times 50\ \text{nm}^2$ up to 4:36, and $100 \times 100\ \text{nm}^2$ up to 21:01. Although the measurement points are sparse after 4:00, STM scans were done at an almost constant rate of one scan per $\sim 40\ \text{s}$. At the missing points, the scanned data were not preserved. According to the data, the growth rate does not have a strong correlation to the scanned area. Hence, we insist the measured growth processes, except for the absolute growth rate, were not very much affected by the measurement, i.e., the anisotropic and nonmonotonic growth rate that was affected by the surface defects, and the growth mode transition from area oriented to height oriented due to the accumulation of stress arising from the lattice mismatch are intrinsic behaviors of the Ag/Si(001) system, although the absolute growth rate might be affected by the heating effect and the long-range interaction from the probe.

Finally, we point out that the unique growth mode of the Ag 3D island without Ag deposition provided a good opportunity to observe the initial growth of a metal 3D island on a semiconductor. In contrast, when a similar experiment is done by supplying metal atoms by deposition during the growth, the density of the metal atoms on the substrate will be quite anisotropic because the STM tip blocks the molecular beam, dropping a shadow on the surface. Our result in the present study is free from such artifacts, i.e., there, the metal atoms were completely isotropically supplied. Thus, the observed anisotropic growth is indeed the characteristic nature of the island.

IV. SUMMARY

The nucleation and initial growth of a Ag 3D island was observed *in situ* by STM on an atomically resolved Si(001) substrate at room temperature. Before the nucleation, the surface was covered by the Ag 2D layer and density of the free Ag atoms and clusters were diffusing over the 2D layer. Just before the nucleation, a Ag cluster with a circular footprint and a diameter of 1.6 nm and height of 2 ML was observed moving around in the vicinity of the nucleation position. When the cluster grew to a lateral dimension of 2.6 nm and a height of 3 ML, it became the nucleus of the island. Since the nucleation process turned out to be affected by the perturbation from the STM probe, the observed size of the nucleus is regarded as the upper limit of the intrinsic value without a measurement effect. During the next 20 min, the growth of the island to a size of $25\ \text{nm} \times 35\ \text{nm} \times 22\ \text{ML}$ was observed to be quite anisotropic and nonmonotonic. The island changed its growth direction frequently, having a rather irregular shape in its footprint, to avoid the surface defects and atomic steps on the substrate. It was also observed that the island does not always extend its boundary and sometimes part of its footprint shrinks to minimize the total free energy of the system. Such quite dynamic behavior of the island shape was explained by the active exchange of Ag atoms among three different phases of (1) the 2D layer phase, (2) the 2D

gas phase of the free Ag atoms diffusing over the 2D layer, and (3) the 3D island phase. The island was a single crystal of Ag that had a crystal orientation of Ag(111)//Si(001) and Ag[1-10]//Si[110]. While the island was still small, the area and the height of the island increased almost linearly as a function of time. When the island grew to ~ 25 nm along Si[1-10] and ~ 35 nm along Si[110], the increase of the area reached saturation because of the accumulation of stress due to the lattice mismatch between the substrate and the island. The anisotropic footprint elongated along Si[110] was consistent with the anisotropic lattice mismatch. On the other hand, the height of the island increased linearly, up to at least 22 ML. Consequently, the number of Ag atoms in the island increased at first as a square function and then as a linear function. The grown island had rather linear edges in its footprint along the

close-packed direction of the Ag(111) crystal. The top surface of the island was almost flat except for the slightly beveled edges.

During the observation, no additional Ag deposition was done. Instead, the island spontaneously grew, absorbing the Ag atoms from the 2D layer phase and the 2D gas phase. The unwetting of the 2D layer in the vicinity of the island was not noticeable, either because the As atoms were provided from a very wide area or because a large part of the Ag atoms came from the 2D gas phase.

Although the observed growth process was affected by the interaction between the STM tip and the diffusing Ag atoms to some degree, the present result provided a concrete picture of the very early stage of the epitaxial growth of a 3D metal island on a semiconductor surface.

*takeuchi@bk.tsukuba.ac.jp

¹E. Bauer, *Rep. Prog. Phys.* **57**, 895 (1994).

²B. Q. Li, W. Swiech, J. A. Venables, and J. M. Zuo, *Surf. Sci.* **569**, 142 (2004).

³B. Q. Li and J. M. Zuo, *Phys. Rev. B* **72**, 085434 (2005).

⁴J. Nogami, *Surf. Rev. Lett.* **1**, 395 (1994).

⁵F. C. H. Luo, G. G. Hembree, and J. A. Venables, in *Evolution of Thin Film and Surface Microstructure*, edited by C. V. Thompson, J. Y. Tsao, and D. J. Srolovitz (Materials Research Society, Pittsburgh, 1991).

⁶A. Samsavar, E. S. Hirschorn, F. M. Leibsle, and T.-C. Chiang, *Phys. Rev. Lett.* **63**, 2830 (1989).

⁷Y. Kimura and K. Takayanagi, *Surf. Sci.* **276**, 166 (1992).

⁸J. C. Glueckstein, M. M. R. Evans, and J. Nogami, *Phys. Rev. B* **54**, R11066 (1996).

⁹T. Tanikawa, I. Matsuda, T. Nagao, and S. Hasegawa, *Surf. Sci.* **493**, 389-398 (2001).

¹⁰A. Zangwill, *Physics at Surfaces* (Cambridge University Press, Cambridge, U.K., 1988).

¹¹T. Hashizume, R. J. Hamers, J. E. Demuth, K. Markert, and T. Sakurai, *J. Vac. Sci. Technol. A* **8**, 249 (1990).

¹²X. F. Lin, K. J. Wan, and J. Nogami, *Phys. Rev. B* **47**, 13491 (1993).

¹³D. Winau, H. Itoh, A. K. Schmid, and T. Ichinokawa, *Surf. Sci.* **303**, 139 (1994).

¹⁴Unpublished.

¹⁵A. Brodde, D. Badt, S. Tosch, and H. Neddermeyer, *J. Vac. Sci. Technol. A* **8**, 251 (1990).

¹⁶K.-J. Kong, H. W. Yeom, D. Y. Ahn, H. Yi, and B. D. Yu, *Phys. Rev. B* **67**, 235328 (2003).

¹⁷There may also be some types of defects that do not prevent the growth of the 3D islands, although most defects do, because the small Ag cluster indicated by the white arrow in Fig. 1(b) was found on a defect on the substrate.

¹⁸D. M. Eigler and E. K. Schweizer, *Nature (London)* **344**, 524 (1990); L. Bartels, G. Meyer, and K.-H. Rieder, *Phys. Rev. Lett.* **79**, 697 (1997).

¹⁹O. Takeuchi, M. Kageshima, H. Sakama and A. Kawazu, *Jpn. J. Appl. Phys.* **40**, 4414 (2001).